Nanoindentation and Molecular Simulation Study of Chemical Doped-Induced Stiffening of a Poly (*p*-phenylene vinylene) Film

JING XU[1]*, GANG XU[1], XIAOJU LONG[1], TINGTING LIU[1] AND HAI XU[2]

[1]*Northeast Petroleum University, Qinhuangdao 066004 PR China*

[2]*College of Chemistry, Jilin University, Changchun, 130021 PR China*

ABSTRACT

A combined experiment and molecular simulation study was performed to understand the mechanism of mechanical change in doped poly (p-phenylene vinylene) (PPV) film. PPV with a partial quinoid structure was obtained using oxidation of ferric chloride. Its chemical structure was determined by FT-IR, Raman and UV-vis spectra. The nanomechanical properties of the neutral PPV film and the chemical-doped PPV films were investigated by nanoindentation test. The critical bending radius of films based on the flexible base was evaluated from the results of the nanoindentation test. The relationship between the benzoid/quinoid ratio of PPV and its inter-molecule interaction was investigated with molecular simulation and the changes of the geometry of PPV single chain and the cohesive energy density (CED) of the multi-PPV. The result suggests that the quinoid PPV has higher CED and rigid chain structures.

KEYWORDS: *PPV, benzoid/quinoid, mechanical properties, CED, inter-molecule interaction*

1. INTRODUCTION

PPV and its derivatives are the most promising and versatile candidates for organic electronic applications due to their commercial availability, low cost and optical-electronic properties that can be tuned over a wide range via judicious functionalization[1-4]. Importantly, PPV and its derivatives have typical semiconductor characteristics, and chemically-doped PPV shows obvious conductor characteristics. The former continue to receive considerable attention for applications such as light emitting diodes, solar cells and field effect transistors [5-7], while the latter may be a candidate for conductive materials [8]. It is important to examine the mechanical properties of films for

J. Polym. Mater. Vol. **34,** No. 4, 2017, 709-717

Correspondence author e-mail: hqzhang@ysu.edu.cn; 373003762@qq,com

applications in various fields of electronics because the flexibility of polymeric films is one of the most attractive advantages among their inherent characteristics. Although the structure and photophysical properties of the doped PPV film have been studied widely [9-10], few studies have evaluated their mechanical characteristics.

The nanoindentation test is a useful technique for examining the mechanical performances, hardness and elastic modulus of thin films made of metals or ceramics with nanometer scale spatial resolution [11-12]. Recently, the nanoindentation test has also been extended to test soft materials including organic materials and polymers [13-16]. However, organic materials are restricted to polymers whose mechanical properties are often used as important material constants for the design and manufacture of industrial products. We recently examined the elastic and plastic characteristics of the MEH-PPV with different chain conformations of a thin film coated on a quartz substrate using the nanoindentation test [17].

In this study, we reported the structural change and nanomechanical properties of neutral PPV and the chemically doped PPV. We then evaluated the critical bending radius of films based on the flexible base from the obtained data of the nanoindentation test. In addition, cohesive energy density of the benzoid PPV and the quinoid PPV were measured to explain the mechanism behind the mechanical properties.

2. EXPERIMENTAL

2.1 Preparation of PPV

The precursor polymer to the PPV (Figure 1) was prepared following the standard polyelectrolyte Wessling route [18] using a,a-dichloro-p-xylene and tetrahydrothiophene as the starting reactants. The reaction was carried out in methanol with tetrabutylammonium hydroxide as the base catalyst. At the end of the reaction, the reaction is quenched by neutralizing the basic reaction mixture with dilute HCl (aq) (0.5 M) to a pH of 4–6. The precursor polymer is purified by dialysis (molecular weight cut-off, MWCO of 4000) against methanol over 3 days with a daily change of fresh solvent.

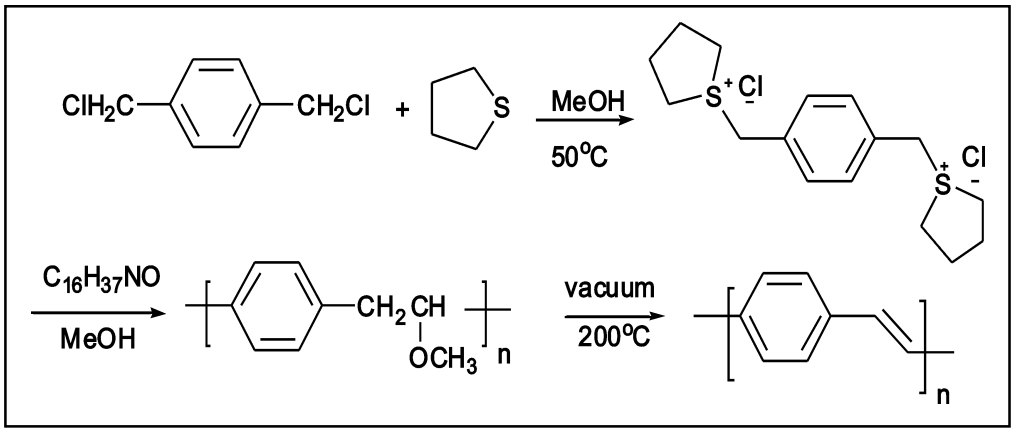

Fig. 1. Synthetic pathways of PPV.

2.2 Neutral PPV film and doped PPV film

PPV precursor films were prepared by spin-coating a water-soluble precursor polyelectrolyte on a quartz substrate, and the PPV precursor film was prepared via pyrolysis at 200°C for 2 hours under vacuum (10^{-3} Torr) to transform them into PPV films. The doped PPV film was performed by immersion in $FeCl_3$ solution as described earlier under nitrogen atmosphere [19].

2.2 Instrument

The FT-IR spectra were recorded on a Perkin-Elmer Spectrum 100 spectrophotometer at frequencies ranging from 400 to 4000 cm^{-1}. The Raman measurements were carried out with a Perkin-Elmer Spectrum 100 spectrophotometer. UV-Vis absorption spectra of the PPV film and the chemical doped PPV film were recorded on a UV-3000 spectrophotometer.

2.3. Nanoindentation

The nanoindentation test was performed using a Hysitron Triboscope (TI-900, USA) with a diamond probe. We used a diamond Berkovich indenter with a tip radius of 450 nm and a maximum load of 50-200 μN, a holding time of 20 s, and loading and unloading rates of 50 μN/s to evaluate Young's modulus and hardness of the neutral PPV film and the doped PPV film. The hardness H of the present material is determined as[20]

$$H=P_{max}/A$$

where P_{max} is the maximum applied load, A is the contact area between the sample and the indenter tip[21].The contact area A is given by $A=24.5h^2$, h is the indentation contact depth. According to oliver and pharr's work, the elastic modulus of the polymer, E is defined by

$$E= (1-\nu^2) [1/ E^*- (1-\nu_i^2) / E_i]^{-1}$$

where ν=0.03 and E are Poisson's ratio and Young's modulus of the material, ν_i(=0.07) and E_i(=1140GP) are the same properties for the indenter, E* is the reduced modulus and it is determined from the following formula[20],

$$E^*= (\pi^{1/2} \beta S) / (2A^{1/2})$$

where S is the measured stiffness of the upper portion of the unloading curve, A is the contact area and β (=1.034) is the shape constant that depends on the geometry of the Berkovich tip.

2.4 Modeling details

Molecular simulation has used molecular mechanics (MM) and molecular dynamics (MD) method in the software of Accelrys Materials Studio v4.4. First, the COMPASS molecular force field was selected to construct a benzoid and quinoid-formed homopolymerization PPV with a periodic boundary condition. This is optimized with MM and MD to an energy minimum. Next, we used an amorphous cell module to build a cubic box (molecule number is 3) with periodic boundary conditions. After optimizing each system energy, the preliminary balance (time: 5 ps) is simulated by MD with NVT constant canonical ensemble. Finally, the constant temperature (298 K) MD simulation was performed, and the cohesive energy density (CED) data analysis was finished with the analysis option in the amorphous cell module.

3. Results and dicussion

3.1. FT-IR and Raman study for the neutral PPV film and the chemical doped PPV film

Figure 2a shows the spectra of the neutral and doped PPV. In the FTIR spectra of neutral PPV, one notes full conversion of the precursor ascertained by the presence of the PPV characteristic bands at 1516, 1423, 962, 837 and 557 cm^{-1} as well as by the absence of the C–S linkage peak at 608 cm^{-1} from tetrahydro-thiophene. Upon oxidation of the PPV film, the infrared spectrum shows new bands at 1556, 1471, 1317, 1153 and 877 cm^{-1}. These bands agree well those reported in Fernandes et al. [9] The emergence of these new bands in the spectra is related to the formation of quinoid structures [22]. Although the formation of the quinoid structure is clear for the doped agents, bands connected with benzoid structure (neutral PPV) survive after doping in the polymer film.

Therefore, we conclude that the polymer is only partially oxidized and the two structures coexist.

Figure 2b shows the Raman spectra of the neutral PPV and doped PPV. The bands at 1545 and 1580 cm^{-1} are attributed to the C=C and C–C stretching of phenyl group in the Raman spectrum of the neutral PPV. The bands at 1627 and 1326 cm^{-1} are assigned to the vinylene C=C stretching and the CC–H bend, respectively. The bands at 1169 and 1418 cm^{-1} are due to the phenyl group CC–H bend and elongation of symmetrical cycle, respectively [22]. In contrast to the neutral PPV, the doped PPV shows shifts in the Raman bands at 1169, 1545, and 1580 cm^{-1}. The vibrational frequency shift at 3, 3 and 5 cm^{-1} for the CC–H bend, the C=C and C–C stretching of phenyl group, respectively. This indicates that the dopant induces structural change in the phenyl group. In addition, the Raman spectra of the doped PPV shows that a new band appears at 1121 cm^{-1}, which agrees well with the quinoid PPV in Fernandes et al. [9]

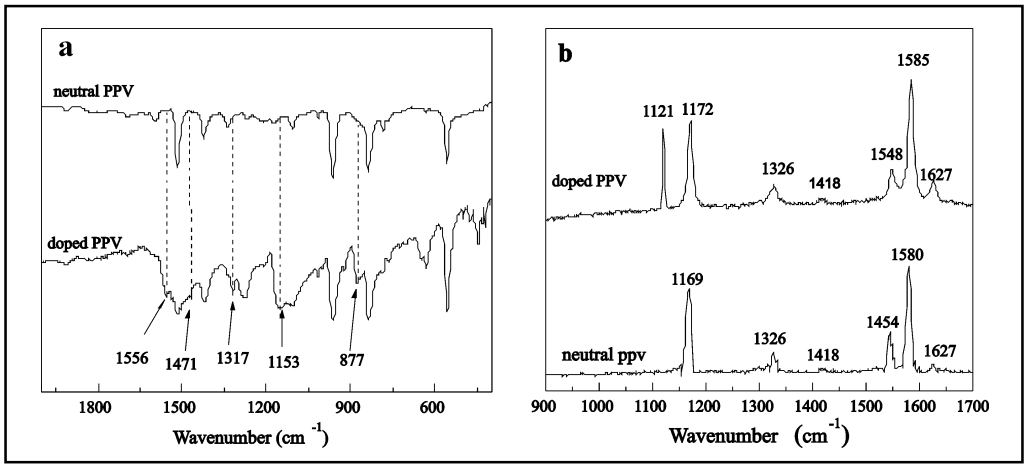

Fig. 2. FT-IR (a) and Raman spectrum (b) of neutral PPV and doped PPV.

3.2. UV–Vis spectra study for the neutral PPV film and the doped PPV film

Figure 3 shows the UV-vis spectra of the neutral PPV and the doped PPV. The UV-Vis spectrum of the PPV shows a broad structure-less absorption between 286-525 nm with a maximum around 426 nm. The result agrees well with the *trans*-PPV in previous studies [23]. A new band appears at 572 nm in the doped PPV film, which is assigned to the π–π^* transition of the quinoid PPV [9]. In addition, the typical absorption band of the PPV still exists in the UV–Vis spectra of the doped PPV indicating the coexistence of quinoid and benzoid structures in doped PPV.

3.3 Mechanical properties of PPV film and doped PPV film

The load-displacement curve of the doped PPV film and neutral PPV film are shown in Figure 4. Generally, the doped PPV was slightly stiffer

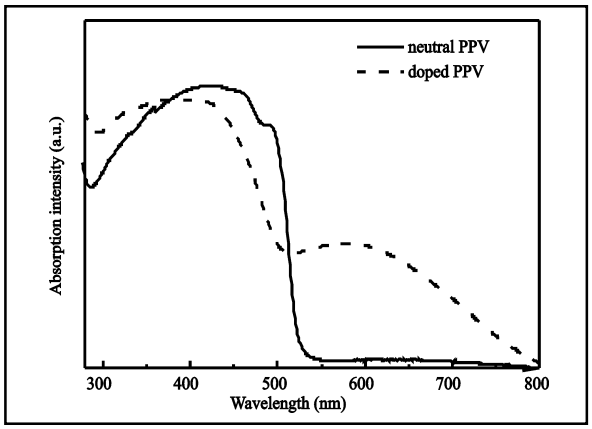

Fig. 3. UV-vis spectra of neutral PPV and doped PPV.

than neutral PPV for any loading rate (Fig. 4) as seen in the decreasing indentation depth at maximum load for doped PPV compared to neutral PPV. For example, the maximum indentation depth in the doped PPV film decreases by 86 nm compared to the neutral PPV film at a load force of 200 μm (A and A'). In other words, the intermolecular interactions in the doped PPV film are stronger than the intermolecular interactions in the neutral PPV film. Furthermore, the doped PPV film and the neutral PPV film show constant creep over 20 seconds (AB=14 nm and A'B'=14 nm, respectively). After unloading, the deformation recovery in the doped PPV film and the neutral PPV film are 112 nm (BC section) and 122 nm (B'C' section), respectively. The lower deformation recovery for the doped PPV film also suggests that the strong intermolecular interaction exits in doped PPV film because the deformation recovery must overcome intermolecular interactions.

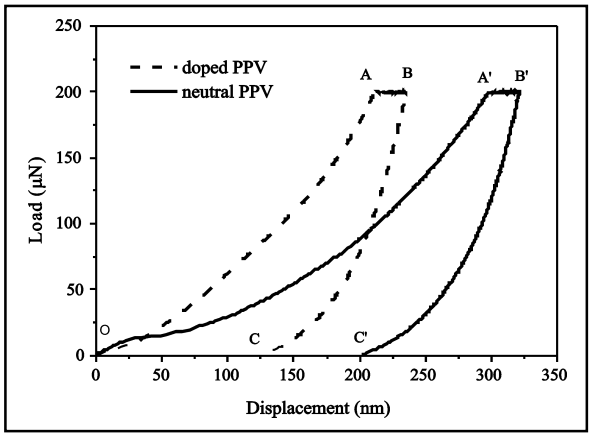

Fig. 4. Load-displacement curves of the neutral PPV doped PPV (Maximal load: 200 μN; Loading rate: 50 μN/s; Holding time: 20 s).

The elastic modulus-load curve and the hardness-load curve of the neutral PPV film and doped PPV film under different loads are shown in Figure 5. The elastic modulus and hardness are nearly constant and range from 50 μN to 200 μN. In contrast with the neutral PPV film, an average elastic modulus of the doped PPV film increases by about 34.23%. The result is consistent with the conclusion of the load-displacement curve. Furthermore, the trend in the hardness is similar to the elastic modulus.

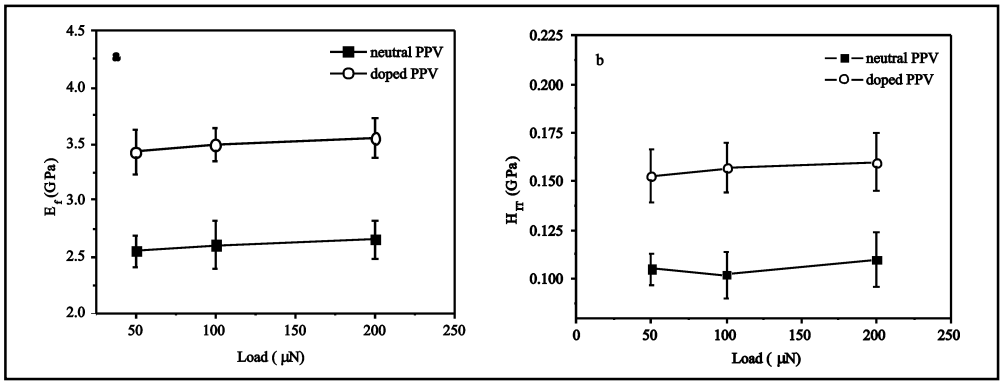

Fig. 5. Elastic modulus-load (a) and hardness-load (b) of the neutral PPV film and doped PPV film under different loads.

3.4 Critical bending radius of the neutral PPV film and doped PPV film

The critical bending radius (r_c) is a critical condition in flexible devices. The mechanical properties obtained with the nanoindentation test are very useful for predicting a critical bending radius r_c. When the organic film is bent into an inner radius r by placing the organic film outside, a bending strain at the top of the organic film is proposed as $\varepsilon=(d_f+d_s)/2r$ [24]. Here, d_f and d_s represent the thicknesses of the organic polymer film and the base film, respectively. Using the relationship $H_{IT}= (2+\pi)/3^{1/2}\sigma_y$ between the indentation hardness and the yield stress σ_y as well as Hook's law ($\varepsilon=\sigma/E$), the critical bending radius is given by

$$r_c = \frac{E_f(2+\pi)(d_f+d_s)}{2\sqrt{3}H_{1T}}$$

Sekitani et al. reported a 50-nm pentacene organic film on a 125-μm base polymer film; the critical bending radius was 4.6 mm [25]. The H_{IT} values and the E_f values of the neutral PPV film and the doped PPV film obtained here were used to calculate materials parameters relative to the pentacene sample. As summarized in Table 1, the predicted critical bending radii of the neutral PPV and doped PPV are 4.59 mm and 4.12 mm, respectively. The predicted critical bending radii are close to the value in the literature, and the slight difference is due to the different organic layer. The result indicates that the predicted critical bending radii from the experimental data of the nano-indentation test are believable. In contrast with the neutral PPV film, the critical bending radii of the doped PPV film decreases 10.2% indicating that the doped PPV thin film can bear a larger bending stress.

TABLE 1. Summary of experimental results. Representative indentation average hardness (HIT) and average Young's modulus (ES) for the films as well as critical bending radius (rc).

	H_{IT} (GPa)	E_f(GPa)	(mm)
Neutral PPV film	0.105	2.60	4.59
Doped PPV film	0.157	3.49	4.12

3.5 Geometries and cohesive energy density of the benzoid /quinoid PPV

Figure 6 shows the conformation of the benzoid/ quinoid PPV of a single chain. There are differences between the geometries of the benzoid/quinoid chains, and after the benzoid chain changes into a quinoid chain, the fluctuation of the chains decreases. The Van der Walls force radius of PPV is affected, and this can change the inter-molecule interaction of PPV directly.

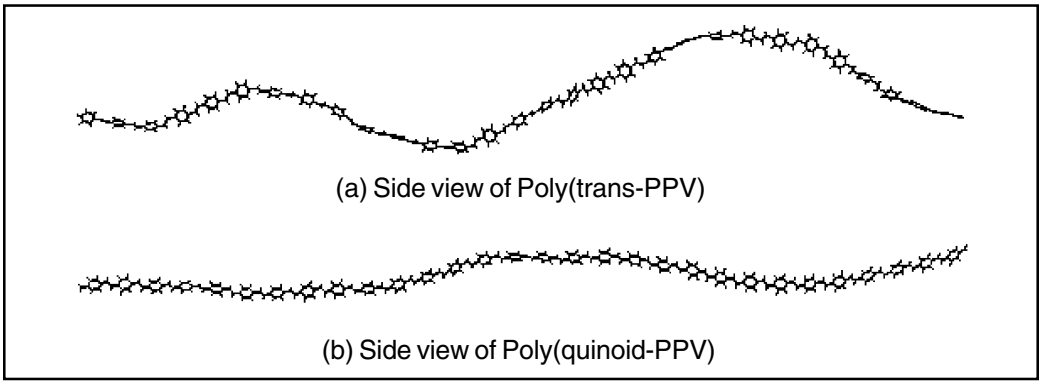

Fig. 6. Conformation of the benzoid /quinoid PPV single chain.

The molecular interactions can be characterized using CED, which is the initial energy derived from the sum of the various attractive forces that hold the molecules of a substance together. The CED of the benzoid and quinoid chain structures of PPV with different degrees of polymerization is obtained by molecular dynamics simulations (Table 2). The CED is decreased with increasing degree of polymerization (Table 2). The CED of the quinoid structure-PPV are always higher than that of the benzoid structure-PPV, and this increase is 39.20% ~91.10%, which indicates that the inter-molecule interaction is enhanced in the quinoid structure-PPV. The conclusions agree with the experimental results.

The cohesive energy density is a physical quantity that evaluates the size of the intermolecular force. The greater the cohesive energy density and the greater the polymer intermolecular force, the greater the cohesive energy density and the greater the mechanical properties of the polymer. To understand the intrinsic factors of the mechanical properties

TABLE 2. CED of the PPV with benzoid (ε_B)/quinoid (ε_Q) chain structure.

Degree of polymerization	ε_Q (J/m^3)	ε_B (J/m^3)	(ε_Q -ε_B) (J/m^3)	(ε_Q -ε_B)/$\varepsilon_{B)}$ %
30	7.17×10^7	5.15×10^7	2.02×10^7	39.22
40	2.99×10^7	1.91×10^7	1.08×10^7	56.54
50	1.47×10^7	7.68×10^6	7.02×10^6	91.40

of benzene PPV and quinone PPV. We used molecular mechanics (MM) and molecular dynamics (MD) method to study the cohesive energy density of benzene PPV and quinone PPV. The results are shown in Table 2. The cohesive energy density of phenone type PPV is greater than that of benzene PPV.

4. CONCLUSIONS

The doped PPV with partial quinoid structre was prepared successfully using oxidation with ferric chloride, and its stucture also was confimed by the FT-IR, Raman and UV-vis spectra. The PPV films with partial quinoid structure shows high hardness and Young's modulus compared to the PPV film with pure benzonoid structure. The quinoid structure result in decrease of critical bending radii. Introduction of the part quinoid structure induced decrease of the cohesive energy density, and weakened interaction between PPV molecules.

Acknowledgements

This work was supported by the National Natural Science Foundation of China (No. 51173155).

REFERENCES

1. Burroughes J, Bradley DDC,Brown AR, Marks RN,Mackay K,Friend RH,Burn PL,Holmes AB (1990) *Nature,* 347:539-541.doi:10.1038/348352a0
2. Pfeiffer SHH, Hörhold HH(1999) *Synthetic Met* 101:109110.doi: 10.1016/s0379-6779(98) 01279-X
3. Ryu H, Subramanian LR, Hanack M(2006) *Tetrahedron* 62:6236–6247.doi:10.1016/ j.tet.2006.04.051
4. Chen JT, Hsu CS (2013) *Polymer,* 54: 4045-4058.doi:10.1016/j.polymer.2013.04.037
5. Jung HJ, Park YJ, Choi SH, Hong JM, Huh J, Cho JH, Kim JH,Park C(2007) *Langmuir* 23:2184-2190.doi:10.1021/la062341h
6. Yue WJ, Wang MT, Nie GJ(2014) *Sol Energy* 99:126-133.doi:10.1016/j.solener.2013.10.040
7. Lee WH, Kong H, Oh SY, Shim HK, Kang IN (2009) *J Polym Sci Pol Chem* 47: 111-120.doi:10.1002/ pola.23126
8. Chen Y, Shih I, Xiao S(2004) *J Appl Phys* 96:454-458.doi: 10.1063/1.1760838
9. Fernandes MR, Garcia JR, Schultz MS, Nart FC(2005) *Thin Solid Films* 474:279-284. doi:10.1016/j.tsf.2004.08.066
10. Baïtoul M, Wéry J, Lefrant S, Faulques E, Buisson JP, Chauvet O(2003) *Phys Rev* B 68:195203-1-195203-6.doi:10.1103/PhysRevB.68.195203
11. Wang F, Huang P, Xu KW(2007) *J Adv Mater special issue:* 2:38-42. dio:10.1016/j.tsf.2006.01.032
12. Chen ZW, Wang X, Bhakhri V, Giuliani F, Atkinson A(2013) *Acta Mater* 61: 5720-5734.doi:10.1016/ j.actamat.2013. 06.016.
13. Kanari M, Kawamata H, Wakamatsu T, Ihara I(2007) *Appl Phys Lett* 90: 061921-1-061921-4. doi:10.1063/1.2472041

14. Tan JC, Furman JD, Cheetham AK(2009) *J Am Chem Soc* 131: 14252–14254. doi:10.1021/ja9060307

15. Kaufman JD, Song J, Klapperich CM (2007) *J Biomed Mater Res* A 81:611-623.doi:10.1002/jbm.a

16. Vapaavuori J, Mahimwalla Z, Chromik RR, Kaivola M, Priimagi A, Barrett CJ (2013) *J Mater chem C* 1:2806-2810.doi:10.1039/C3TC30246F

17. Wang P, Wu LL, Zhang D, Zhang HQ (2013) *B Mater Sci* 36:833-837. Doi:10.1007/s12034-013-0525-5

18. Zeng QG, Ding ZJ, Ju X, Zhang ZM (2005) *Eur Polym J* 41: 743-746.doi: 10.1016/j.eurpolymj.2004.11.010

19. Tzolov M, Koch VP, Bruetting W, Schwoerer M (2000) *Synthetic Met* 109: 85-89.doi:10.1016/S0379-6779(99)00207-6

20. Bahr DF, Hoehn JW, Moody NR, Gerberich WW (1997) *Acta Mater* 45:5163-5175.doi:10.1016/S1359-6454(97)00180-8

21. Fang TH, Chang WJ (2003) *Microelectron Eng* 65:231-238. doi:10.1016/S0167-9317(02)00885-7

22. Lefrant S, Perrin E, Buisson JP, Eckhardt H, Han CC(1989) *Synthetic Met* 29:91-96.doi: 10.1016/0379-6779(89)90281-6

23. Bianchi RF, Gonçalves D (2013) *Mater Chem Phys* 141: 973-978.10.1016/j.matchemphys.2013.06.037

24. Suo Z, Ma EY, Gleskova H, Wagner S (1999) *Appl Phys Lett* 74: 1177-1179.doi:10.1063/1.123478

25. Sekitani T, Kato Y, Iba S, Shinaoka H, Someya T, Sakurai T, Takagi S (2005) *Appl Phys Lett* 86: 073511-073511-3.doi:10.1063/1.1868868

Received: 17-06-2017

Accepted: 14-09-2017